ACS Medicinal Chemistry Letters
Cite This: ACS Med. Chem. Lett. XXXX, XXX, XXX-XXX
Letter
pubs.acs.org/acsmedchemlett

Adding a Hydrogen Bond May Not Help: Naphthyridinone vs Quinoline Inhibitors of Macrophage Migration Inhibitory Factor

Thomas K. Dawson, Pawel Dziedzic, Michael J. Robertson, José A. Cisneros, Stefan G. Krimmer, Ana S. Newton, Julian Tirado-Rives, and William L. Jorgensen*

Department of Chemistry, Yale University, New Haven, Connecticut 06520-8107, United States

Supporting Information

ABSTRACT: Coordination of the ammonium group of Lys32 in the active site of human macrophage migration inhibitory factor (MIF) using a 1,7-naphthyridin-8-one instead of a quinoline is investigated. Both gas- and aqueous-phase DFT calculations for model systems indicate potential benefits for the added hydrogen bond with the lactam carbonyl group, while FEP results are neutral. Three crystal structures are reported for complexes of MIF with **3a**, **4a**, and **4b**, which show that the desired hydrogen bond is formed with O−N distances of 2.8−3.0 Å. Compound **4b** is the most potent new MIF inhibitor with K_i and K_d values of 90 and 94 nM; it also has excellent aqueous solubility, 288 μg/mL. Consistent with the FEP results, the naphthyridinones are found to have similar potency as related quinolines in spite of the additional protein−ligand hydrogen bond.

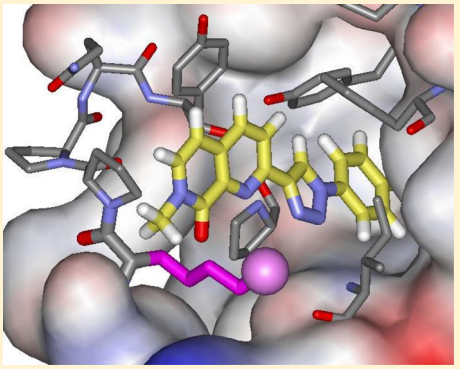

KEYWORDS: *MIF inhibitors, lysine coordination, protein crystallography*

Macrophage migration inhibitory factor (MIF) is a proinflammatory cytokine that is extensively expressed in many mammalian cell types including endothelial cells, macrophages, and T-cells. High MIF levels are associated with numerous inflammatory and neurological disorders including rheumatoid arthritis, atherosclerosis, and Alzheimer's disease.[1−3] MIF also plays a role in cancer through regulation of cell proliferation and promotion of angiogenesis.[4] Consequently, there has been significant activity in searching for inhibitors of MIF signaling,[5] which is initiated by its binding to cell-surface receptors CD74, CXCR2, and CXCR4. Interestingly, MIF also has enzymatic activity as a keto−enol tautomerase, though this role may be vestigial in humans. MIF is a trimeric protein with three active sites that occur at the interfaces of the monomer subunits. Discovery of MIF inhibitors has focused on small molecules that bind to and protrude from the tautomerase active sites causing interference with the receptor activation.[6]

Our laboratory has reported potent MIF tautomerase inhibitors that have arisen from computer-aided design, small-molecule synthesis, performance of inhibition and binding assays, and protein crystallography.[7−10] In particular, a variety of 4-quinolinyltriazoles (**1**, **2**) has been discovered with K_i values in the tautomerase assay below 50 nM,[7,10] which have been confirmed by K_d measurements in a fluorescence polarization assay.[9] In addition, crystal structures were reported for complexes of three of the inhibitors with MIF including for the parent **1** (R = H) and its methoxyethoxy analog, **1** (R = MOEO).

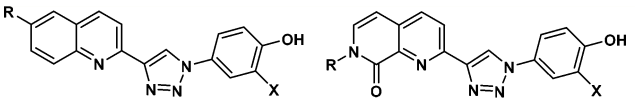

1 (X = H), **2** (X = F) **3** (X = H), **4** (X = F)

The positioning of the latter compound in the MIF tautomerase site is illustrated in Figure 1. In addition to aryl−aryl interactions with Tyr36, Tyr95, and Phe113, hydrogen bonds occur between Asn97 and the phenolic hydroxyl group of the inhibitor, the backbone NH of Ile64 and N2 of the triazole, and the ammonium group of Lys32 with N3 of the triazole, the quinoline nitrogen, and the carbonyl oxygen of Ile64. The triple coordination of Lys32 is striking and can be expected to be augmented by one or two water molecules as the Lys32−Gln35 segment is on the surface of the protein. This follows from prior computations of the hydration of methylammonium ion, which reveal four to five hydrogen bonds with water molecules,[11] and from viewing numerous crystal structures in the RSCB Protein Data Bank. It is often found that the ammonium group of lysine participates in a total of four or five hydrogen bonds with surrounding residues, ligands, and water molecules. A sample illustration is provided in Figure 2 from a crystal structure for an aspartate kinase with lysine itself as a ligand.[12] The ammonium group is seen to engage in five hydrogen bonds with three backbone carbonyl groups, the side-chain carboxylate group of an aspartate residue, and a water molecule.

Received: September 21, 2017
Accepted: November 10, 2017

DOI: 10.1021/acsmedchemlett.7b00384
ACS Med. Chem. Lett. XXXX, XXX, XXX−XXX

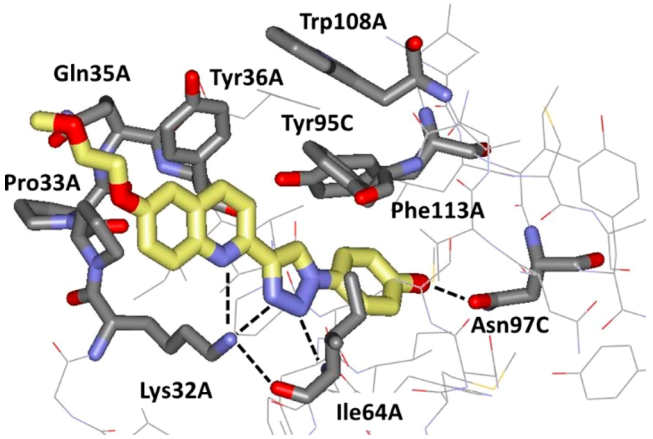

Figure 1. Rendering from the 1.8 Å crystal structure of **1** (R = MOEO) bound to MIF (PDB ID: 4WRB).[7] Carbon atoms of the inhibitor are colored yellow. Hydrogen bonds are highlighted with dashed lines; the methoxyethoxy group on C6 of the quinoline is solvent-exposed.

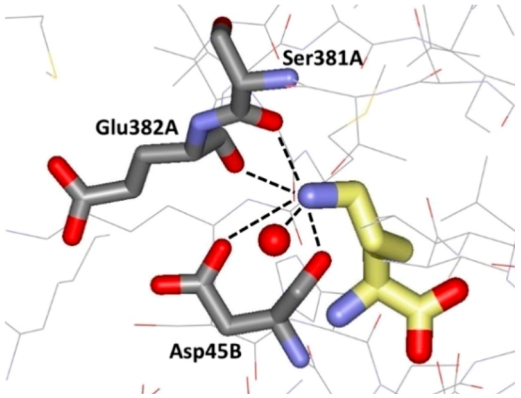

Figure 2. Coordination of a lysine ligand in the crystal structure of a complex with an aspartate kinase (PDB ID: 3AB4).[12] Hydrogen bonds are denoted with dashed lines; the O−N distances going counterclockwise from the top are 2.58, 3.43, 3.51, 2.74, and 2.61 Å.

In view of this pattern, modifications of **1** were sought featuring additional coordination of Lys32 that could enhance the inhibition of MIF's tautomerase activity. In the initial study,[7] addition of a phenoxy group at C8 in the quinoline was considered, but this led to a five-fold reduction in the inhibitory activity compared to the parent **1** (R = H). Substitution of a 4-methoxyphenyl group at C8 to engage in a cation−π interaction with Lys32 was even less successful, while replacement of the quinoline with 1,8-naphthyridine resulted in a 2.5-fold reduction in potency.[7] Another idea is explored here; namely, placement of a carbonyl group at C8 of the quinoline should project closer to Lys32 than N8 of the naphthyridine. Thus, we decided to consider 1,7-naphthyridin-8-ones as in **3** and **4**. Model building with the BOMB program[13] using OPLS force fields[14] provided auspicious images as in Figure 3 for the complex of **3a** (**3**, R = Me) with MIF. The computed structure has hydrogen bonds between Lys32 and the naphthyridinone O and N, N3 of the triazole, and the carbonyl group of Ile64 with lengths of 3.29, 3.33, 3.18, and 2.76 Å, respectively. DFT calculations (B2PLYP-D3BJ/aug-cc-pVTZ//ωB97X-D/6-311G++(d,p))[15,16] were also carried out for model complexes of NH_4^+ with 1,2,3-triazole and the quinolinyl and naphthyridinonyl

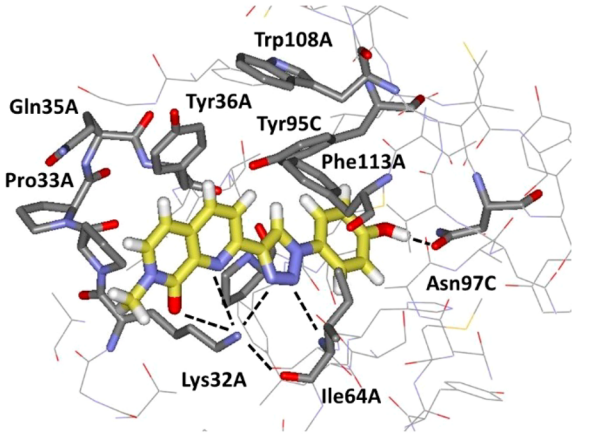

Figure 3. Modeled complex of **3a** with MIF using the BOMB program. Hydrogen bonds are shown with dashed lines.

systems in Figure 4. Gas-phase energy minimizations gave interaction energies of −35.5, −45.1, and −59.1 kcal/mol for

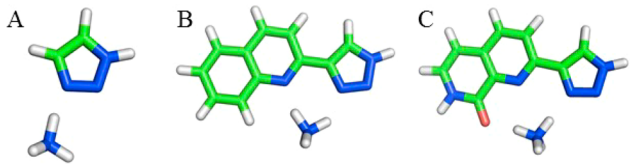

Figure 4. Computed structures for complexes of ammonium ion with (A) 1,2,3-triazole and its (B) quinolinyl and (C) 1,7-naphthyridin-8-onyl analogs. Gas-phase DFT results give interaction energies of −36, −45, and −59 kcal/mol for A, B, and C.

the three complexes. Effects of hydration were then approximated using a polarizable continuum model (IEFPCM),[17] yielding interaction energies of −9.9, −11.7, and −17.6 kcal/mol. We also ran Monte Carlo free-energy perturbation (FEP) calculations at 25 °C for the conversion of **3a** to **1a** (**1**, R = H) in TIP4P water both unbound and bound to MIF using standard protocols,[7,13] including the OPLS-AA/M force field for MIF and OPLS/CM1A for the inhibitors.[14,18] The FEP calculations were run twice with somewhat different initial geometries for the complex; the two results both predict a slightly more favorable free energy of binding for **3a** by 0.28 ± 0.32 and 0.45 ± 0.32 kcal/mol. Such differences are too small to translate into a clear experimental effect.[14]

With this ambiguity, we endeavored to resolve the matter by synthesizing **3** and **4** with R = Me (**3a**, **4a**) and CH_2COOH (**4b**). The key intermediates are the acetylenes **13**/**14** in Scheme 1, which are converted to the desired products via one-

Scheme 1. Synthesis of the Acetylenic Intermediates

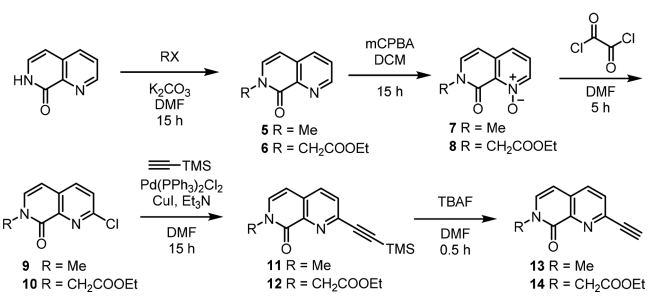

DOI: 10.1021/acsmedchemlett.7b00384
ACS Med. Chem. Lett. XXXX, XXX, XXX−XXX

pot Cu(I)-catalyzed click reactions.[7] Starting from commercially available 1,7-naphthyridin-8(7*H*)-one, alkylation with methyl iodide or ethyl-2-bromoacetate provides **5**/**6**, which after mCPBA oxidation and treatment with oxalyl dichloride yields the 2-chloro-naphthyridinones **9**/**10**. A Sonogashira coupling followed by removal of the TMS protecting group delivers the desired compounds **13**/**14**. For **4b**, the ethyl ester was hydrolyzed with NaOH in dioxane as the final step. Full details are provided in the Supporting Information.

As also detailed in the Supporting Information, we obtained cocrystal structures for **3a**, **4a**, and **4b** bound to MIF at resolutions of 1.17, 2.16, and 2.00 Å. The structures are all similar for the binding sites; for **4a**, Figure 5 illustrates the four

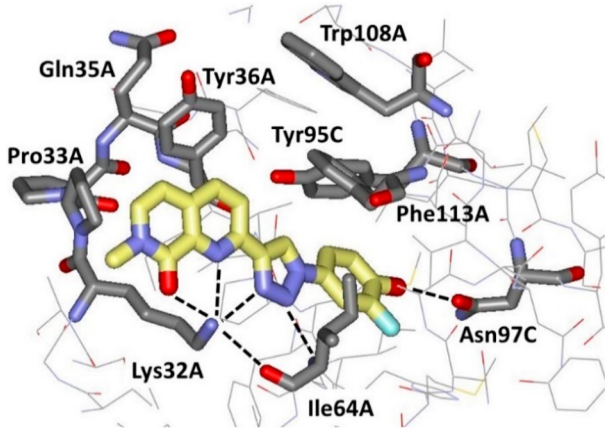

Figure 5. Rendering from the 2.16 Å crystal structure of **4a** bound to MIF (PDB ID: 6B1C).

expected hydrogen bonds to Lys32. The structures for **4a** and **4b** also confirm that the fluorine atom points between Ile64 and Asn97.[9] In the 1.17 Å structure for **3a**, all three binding sites for the MIF trimer are occupied. In one copy, the O-Lys N or N-Lys N distances are 2.94, 3.16, 2.95, and 2.82 Å for the naphthyridinone O and N, triazole N, and Ile64 oxygen atom, and in the other copies, they are 2.83, 3.13, 3.03, 2.80 Å and 3.04, 3.23, 3.03, 3.34 Å. Thus, there are small differences associated with variations in the interprotein packing. No hydrogen-bonded water molecules are resolved for Lys32, while there is one 2.83 Å from the naphthyridinone oxygen atom.

For the assaying, inhibition constants K_i were determined as before using 4-hydroxyphenylpyruvic acid (HPP) as the substrate.[7,8] Inhibitory activity is monitored by measuring formation of the borate complex of the enol product at 305 nm using a Tecan Infinite F500 plate reader. Binding constants K_d were also obtained for the new compounds using a fluorescence polarization assay, which has been fully detailed.[9] In addition, the aqueous solubility of **4b** was measured with a shake-flask procedure.[7,10,19] Saturated solutions in Britton−Robinson buffer (pH 6.5) are filtered (Acrodisc syringe, 0.2 μm pore) and analyzed by UV−vis spectroscopy (Agilent 8453).

The assay results for the naphthyridinones are compared with data for previously reported analogs of **1** and **2** and a reference compound, (*R*)-ISO-1,[20] in Table 1. For (*R*)-ISO-1, K_i measurements have been made nine times with results of 21−39 μM and an average of 30 μM, while K_d measurements have been made four times with results of 20−30 μM, averaging 23 μM. The K_i and K_d results in Table 1 are in good accord

Table 1. Experimental Inhibition Constants K_i, Binding Constants K_d (μM), and Aqueous Solubility S (μg/mL)

compd	R	K_i	K_d	S
1a	H	0.23	0.26	2.2
1b	$HOCH_2CH_2O$	0.53	ND	2.6
1c[a]	$H_2NCH_2CH_2O$	0.26	ND	3.7
1d[a]	$H_2N(CH_2CH_2O)_2$	0.36	0.35	13.9
1e[b]	4-Mr$(CH_2CH_2O)_2$	0.16	0.21	48.5
1f	$HOOCCH_2O$	0.20	ND	365
2a[a]	$H_2N(CH_2CH_2O)_2$	0.144	0.16	9.1
2b	4-Mr$(CH_2CH_2O)_2$	0.074	0.15	27.2
2c	$HOOCCH_2O$	0.048	ND	37.0
2d	$HOOC(CH_2)_3O$	0.039	0.063	19.2
3a	H_3C	0.363	0.213	ND
4a	H_3C	0.075	0.111	ND
4b	$HOOCCH_2$	0.090	0.094	288
(*R*)-ISO-1		30.1	23.1	ND

[a]TFA salt. [b]M_r = morpholinyl.

with the differences, consistent with the expected uncertainties for both measurements.

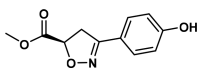

(*R*)-ISO-1

Comparison of the results for **1a** and **3a** shows that the two compounds have essentially the same activity. Though **3a** represents an improvement over the previous modifications of the quinoline fragment,[7] it is provocative in view of the added hydrogen bond to Lys32 that is well-documented in the crystal structures. Other analogs of **1a** also typically have K_i and K_d values between 0.2 and 0.4 μM (Table 1). Addition of the fluorine in progressing from **1** to **2** usually improves activity two- to four-fold, as for **1d**, **1e**, and **1f** vs. **2a**, **2b**, and **2c**. The effect is attributed to enhanced strength of the hydrogen bond between the phenolic hydroxyl group and Asn97 as well as hydrophobic contact of the fluorine with the side chain of Met101.[7] The five-fold enhancement in K_i and two-fold enhancement in K_d for **3a** vs. **4a** suggests that the K_i for **3a** in Table 1 is somewhat too high. In any event, **4a** and **4b** are very potent MIF tautomerase inhibitors with K_is of 75 and 90 nM. These activities are again similar to those for analogs of **2** in spite of the added hydrogen bond with Lys32 (Figure 5). It may be noted that the carboxylic acid **4b** was chosen for synthesis since there seemed to be a pattern favoring expected placement of the carboxylate group near Lys32 as in **2c** and **2d** vs **2a** and **2b**; however, the electrostatic benefit is not apparent for **4a** vs **4b**, perhaps owing to the proximity of the naphthyridinone carbonyl group.

Though the FEP results turned out to be qualitatively correct, the confidence level is not yet at the point where one rejects pursuit of analogs as tempting as **3** and **4**. Traditional scoring functions used in docking calculations typically count well-formed protein−ligand hydrogen bonds like the present cases as contributing 1 kcal/mol (a factor of 5) to binding affinity.[21,22] Thus, the outcome is context dependent, being sensitive to the complex balance of protein−ligand, protein−water, and ligand−water interactions. In viewing complexes for **1a** and **3a** from the Monte Carlo simulations, one might expect one less hydrogen bond between water molecules and Lys32 for **3a**. However, for both **1a** and **3a**, there are consistently two water molecules hydrogen-bonded to Lys32, and for **3a**, there is

DOI: 10.1021/acsmedchemlett.7b00384
ACS Med. Chem. Lett. XXXX, XXX, XXX−XXX

an additional hydrogen bond with the naphthyridinone carbonyl group (Figure 6). For the unbound **3a**, there is also just one water molecule hydrogen-bonded to the carbonyl group. Thus, the origins of the presumably greater dehydration penalty upon binding **3a** rather than **1a**, which offsets the added protein−ligand hydrogen bond with **3a**, are subtle and likely dominated by entropy effects.[23]

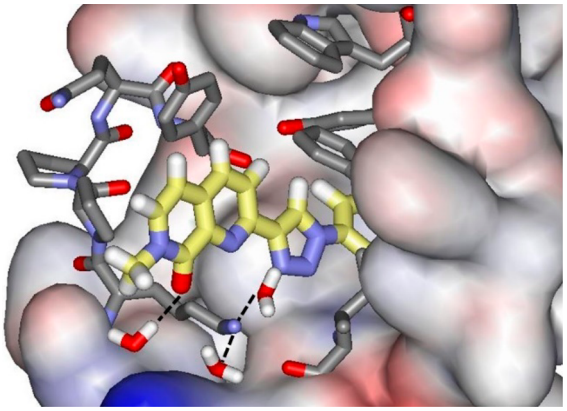

Figure 6. Illustration from a Monte Carlo simulation of **3a** showing two water molecules hydrogen-bonded with Lys32 and one with the carbonyl group of **3a**. Lys32 is participating in a total of six hydrogen bonds.

Though clear enhancement of potency was not found with the naphthyridinones, they do provide an alternative chemotype for potent MIF inhibitors. Prospects for further advancement of **4b** were increased by determining that it also has excellent aqueous solubility at 288 μg/mL (Table 1). In addition, the study has provided an informative lesson on the subtleties of lead optimization.

■ ASSOCIATED CONTENT

Supporting Information

The Supporting Information is available free of charge on the ACS Publications website at DOI: 10.1021/acsmedchemlett.7b00384.

Synthetic procedures, NMR and HRMS spectral data for all new compounds, crystallographic details, and complete citation for ref 16 (PDF)

Accession Codes

The crystal structures for the complexes of **3a**, **4a**, and **4b** with MIF have been deposited in the RSC Protein Data Bank with IDs 6B1K, 6B1C, and 6B2C.

■ AUTHOR INFORMATION

Corresponding Author

*E-mail: william.jorgensen@yale.edu.

ORCID

Julian Tirado-Rives: 0000-0001-7330-189X

William L. Jorgensen: 0000-0002-3993-9520

Notes

The authors declare no competing financial interest.

■ ACKNOWLEDGMENTS

Gratitude is expressed to the National Institutes of Health (GM32136) for research support, to the National Science Foundation for a fellowship for M.J.R. (DGE-1122492), and to Drs. Thomas Steitz, Michael Strickler, and Yong Xiong for assistance at the Yale Richards Center. This work used the NE-CAT 24-ID-C and 24-ID-E beamlines (GM103403) and Pilatus detector (RR029205) at the APS (DE-AC02-06CH11357).

■ ABBREVIATIONS

DFT, density functional theory; FEP, free-energy perturbation; DCM, dichloromethane; DMF, dimethylformamide; TBAF, tetrabutylammonium fluoride

■ REFERENCES

(1) Garai, J.; Lorand, T. Macrophage Migration Inhibitory Factor (MIF) Tautomerase Inhibitors as Potential Novel Anti-Inflammatory Agents: Current Developments. *Curr. Med. Chem.* **2009**, *16*, 1091−1114.

(2) Asare, Y.; Schmitt, M.; Bernhagen, J. The vascular biology of macrophage migration inhibitory factor (MIF) Expression and effects in inflammation, atherogenesis and angiogenesis. *Thromb. Haemostasis* **2013**, *109*, 391−398.

(3) Leyton-Jaimes, M. F.; Kahn, J.; Israelson, A. Macrophage migration inhibitory factor: A multifaceted cytokine implicated in multiple neurological diseases. *Exp. Neurol.* **2017**, DOI: 10.1016/j.expneurol.2017.06.021.

(4) Nobre, C.C. G.; Galvão de Araújo, J. M.; Fernandes, T. A. A. M.; Cobucci, R. N. O.; Lanza, D. C. F.; Andrade, V. S.; Fernandes, J. V. Macrophage Migration Inhibitory Factor (MIF): Biological Activities and Relation to Cancer. *Pathol. Oncol. Res.* **2017**, *23*, 235−244.

(5) Xu, L.; Li, Y.; Sun, H.; Zhen, X.; Qiao, C.; Tian, S.; Hou, T. Current developments of macrophage migration inhibitory factor (MIF) inhibitors. *Drug Discovery Today* **2013**, *18*, 592−600.

(6) Pantouris, G.; Syed, M. A.; Fan, C.; Rajasekaran, D.; Cho, T. Y.; Rosenberg, E. M., Jr; Bucala, R.; Bhandari, V.; Lolis, E. An analysis of MIF structural features that control functional activation of CD74. *J. Chem. Biol.* **2015**, *22*, 1197−1205.

(7) Dziedzic, P.; Cisneros, J. A.; Robertson, M. J.; Hare, A. A.; Danford, N. E.; Baxter, R. H.; Jorgensen, W. L. Design, Synthesis, and Protein Crystallography of Biaryltriazoles as Potent Tautomerase Inhibitors of Macrophage Migration Inhibitory Factor. *J. Am. Chem. Soc.* **2015**, *137*, 2996−3003.

(8) Cisneros, J. A.; Robertson, M. J.; Valhondo, M.; Jorgensen, W. L. Irregularities in enzyme assays: The case of macrophage migration inhibitory factor. *Bioorg. Med. Chem. Lett.* **2016**, *26*, 2764−2767.

(9) Cisneros, J. A.; Robertson, M. J.; Valhondo, M.; Jorgensen, W. L. A Fluorescence Polarization Assay for Binding to Macrophage Migration Inhibitory Factor and Crystal Structures for Two Potent Inhibitors. *J. Am. Chem. Soc.* **2016**, *138*, 8630−8638.

(10) Cisneros, J. A.; Robertson, M. J.; Mercado, B. Q.; Jorgensen, W. L. Systematic Study of Effects of Structural Modifications on the Aqueous Solubility of Drug-like Molecules. *ACS Med. Chem. Lett.* **2017**, *8*, 124−127.

(11) Jorgensen, W. L.; Gao, J. Monte Carlo Simulations of the Hydration of Ammonium and Carboxylate Ions. *J. Phys. Chem.* **1986**, *90*, 2174−2182.

(12) Yoshida, A.; Tomita, T.; Kuzuyama, T.; Nishiyama, M. Mechanism of concerted inhibition of $\alpha_2\beta_2$-type heterooligomeric aspartate kinase from *Corynebacterium glutamicum*. *J. Biol. Chem.* **2010**, *285*, 27477−27486.

(13) Jorgensen, W. L. Efficient Drug Lead Discovery and Optimization. *Acc. Chem. Res.* **2009**, *42*, 724−733.

(14) Jorgensen, W. L.; Tirado-Rives, J. Potential energy functions for atomic-level simulations of water and organic and biomolecular systems. *Proc. Natl. Acad. Sci. U. S. A.* **2005**, *102*, 6665−6670.

(15) Goerigk, L.; Grimme, S. A thorough benchmark of density functional methods for general main group thermochemistry, kinetics, and noncovalent interactions. *Phys. Chem. Chem. Phys.* **2011**, *13*, 6670−6688.

(16) Frisch, M. J.; Trucks, G. W.; Schlegel, H. B.; Scuseria, G. E.; Robb, M. A.; Cheeseman, J. R.; Scalmani, G.; Barone, V.; Mennucci,

DOI: 10.1021/acsmedchemlett.7b00384
ACS Med. Chem. Lett. XXXX, XXX, XXX−XXX

B.; Petersson, G. A.; et al. *Gaussian 09*, revision D.01; Gaussian, Inc.: Wallingford, CT, 2009.
(17) Cancès, E.; Mennucci, B.; Tomasi, J. A new integral equation formalism for the polarizable continuum model: Theoretical background and applications to isotropic and anisotropic dielectrics. *J. Chem. Phys.* **1997**, *107*, 3032−3041.
(18) Robertson, M. J.; Tirado-Rives, J.; Jorgensen, W. L. Improved Peptide and Protein Torsional Energetics with the OPLS-AA Force Field. *J. Chem. Theory Comput.* **2015**, *11*, 3499−3509.
(19) Baka, E.; Comer, J. E. A; Takács-Novák, K. Study of equilibrium solubility measurement by saturation shake-flask method using hydrochlorothiazide as model compound. *J. Pharm. Biomed. Anal.* **2008**, *46*, 335−341.
(20) Lubetsky, J. B.; Dios, A.; Han, J.; Aljabari, B.; Ruzsicska, B.; Mitchell, R.; Lolis, E.; Al-Abed, Y. The tautomerase active site of macrophage migration inhibitory factor is a potential target for discovery of novel anti-inflammatory agents. *J. Biol. Chem.* **2002**, *277*, 24976−24982.
(21) Eldridge, M. D.; Murray, C. W.; Auton, T. R.; Paolini, G. V.; Mee, R. P. Empirical scoring functions: I. The development of a fast empirical scoring function to estimate the binding affinity of ligands in receptor complexes. *J. Comput.-Aided Mol. Des.* **1997**, *11*, 425−445.
(22) Böhm, H.-J. Prediction of binding constants of protein ligands: A fast method for the prioritization of hits obtained from de novo design or 3D database search programs. *J. Comput.-Aided Mol. Des.* **1998**, *12*, 309−323.
(23) Krimmer, S. G.; Betz, M.; Heine, A.; Klebe, G. Methyl, Ethyl, Propyl, Butyl: Futile But Not for Water, as Correlation of Structure and Thermodynamic Signature Shows in a Congeneric Series of Thermolysin Inhibitors. *ChemMedChem* **2014**, *9*, 833−846.

DOI: 10.1021/acsmedchemlett.7b00384
ACS Med. Chem. Lett. XXXX, XXX, XXX−XXX